Nuclear Engineering and Technology 57 (2025) 103851

Contents lists available at ScienceDirect

Nuclear Engineering and Technology

journal homepage: www.elsevier.com/locate/net

Original Article

Optimal ferro frit for leaching stability of radioactive metal oxide sludges-based solidified body

Ki Joon Kang [a,1], Sia Hwang [b,1], Hee Reyoung Kim [b,*]

[a] Radioactive Waste Radiochemical Analysis Section, Korea Atomic Energy Research Institute (KAERI), Daejeon, 34057, Republic of Korea
[b] Department of Nuclear Engineering, Ulsan National Institute of Science and Technology (UNIST), Ulsan, 44919, Republic of Korea

ARTICLE INFO

Keywords:
Radioactive waste
Solidification
Ferro frit
Oxide sludge
Waste disposal

ABSTRACT

In nuclear power plants, the corrosion of metallic components exposed to radioactive liquid waste and coolant can result in the formation of sludge. This study examined the optimization of ferro frit additives to enhance the leaching stability of solidified radioactive sludge. Specifically, simulated sludge, composed of Fe_2O_3, Cr_2O_3, NiO, and Co, was solidified using various additives—including ferro frit 3110, ferro frit 3195, and B_2O_3—and evaluated for leaching stability under ANSI/ANS 16.1 conditions. Among the four target elements, Fe, Ni, and Co consistently demonstrated excellent leaching resistance, while Cr required further immobilization. Co, a key nuclide in leaching resistance assessments for radioactive waste disposal, exhibited low leachate concentrations under all tested conditions. The addition of B_2O_3-rich frits substantially improved Cr leaching resistance by strengthening the glass network structure and suppressing ionic mobility. This improvement is attributed to B_2O_3's role in reducing non-bridging oxygen content and increasing network polymerization. As the Cr_2O_3 and NiO content in the sludge increased, the sintering temperature required for stable solidification rose from 950 to 1050 °C. These findings demonstrate that producing chemically durable solidified radioactive sludge suitable for final disposal requires both thermal and compositional optimization, particularly through the incorporation of B_2O_3.

1. Introduction

Dried sludge waste typically consists of fine particles, which increases the risk of radionuclide migration in the sludge disposal environment. Consequently, solidifying sludge waste is essential to immobilize these particles before final disposal. To date, various methods have been developed to effectively solidify homogeneous radioactive waste and thus enhance its safety and containment efficiency. In the case of sludge waste, the substances of interest primarily include oxides formed through the corrosion of metallic structures in nuclear power plants (NPPs), including Fe oxide (Fe_2O_3), Ni oxide (NiO), and Cr(III) oxide (Cr_2O_3). These oxides commonly originate from stainless steel components [1,2]. However, the high melting points of most of these oxides present considerable challenges for complete melting. To address this issue, various additives have been introduced into radioactive waste to facilitate solidification. Based on this principle, several solidification techniques have been employed, including vitrification, asphalt solidification, cement solidification, and polymer solidification. Among these, cement curing with water is the most widely used approach. Nevertheless, these conventional techniques often yield products that are unstable at elevated temperatures and tend to produce large solidified volumes, thereby reducing disposal efficiency and increasing overall cost.

A key advantage of the cement curing technique is its ability to achieve solidification at ambient temperatures. However, this benefit is offset by cement's susceptibility to thermal degradation. Studies reveal that ettringite, a key component of cement, begins to decompose at approximately 70 °C, suggesting that cement-based waste forms may degrade even under relatively mild thermal conditions [3]. In comparison, polymers offer greater thermal stability, maintaining structural integrity at temperatures up to 100 °C. However, polymer solidification typically requires the addition of 40–45 % auxiliary additives, which results in a solidified waste volume approximately 1.7 times greater than that of the original waste [4]. Similar thermal limitations are observed in asphalt solidification. Specifically, given the low thermal stability of asphalt (≈180 °C), its solidification is unsuitable for high-temperature

* Corresponding author. Department of Nuclear Engineering, Ulsan National Institute of Science and Technology (UNIST), Ulsan, 44919, Republic of Korea.
E-mail addresses: kjkang7024@kaeri.re.kr (K.J. Kang), siahwang@unist.ac.kr (S. Hwang), kimhr@unist.ac.kr (H.R. Kim).
[1] These authors contributed equally to this work.

https://doi.org/10.1016/j.net.2025.103851
Received 22 February 2025; Received in revised form 24 May 2025; Accepted 11 August 2025
Available online 11 August 2025

applications [5]. Thus, because asphalt is prone to heat-induced damage, it is vulnerable to degradation at elevated temperatures, posing a serious risk in the event of a fire at a radioactive waste disposal facility. In contrast, the vitrification process yields products with enhanced thermal stability. It operates at temperatures exceeding 1100 °C, producing a more thermally stable waste form. To aid the solidification of materials with melting points above 2000 °C, a substantial amount of glass—melting at 1100–1300 °C—is incorporated into the mixture. In particular, glasses containing B_2O_3 exhibit low glass transition temperatures, creating a favorable thermal environment for radioactive waste solidification. Additionally, appropriate amounts of B_2O_3 have been reported to improve the mechanical strength of low-temperature glass-ceramics [6].

The maximum waste loading capacity of vitrification typically ranges from 20 to 30 % [7]; however, it can increase to 45 % depending on the waste composition [8]. In the vitrification process, a mixture of waste and glass is melted to form a stable, durable matrix suitable for long-term hazardous waste management. Consequently, pressureless vitrification requires a large quantity of glass powder, which increases the volume of the solidified radioactive waste relative to that of the original radioactive waste. To mitigate this, researchers have explored alternative approaches for specific waste types. For instance, studies have demonstrated that clinoptilolite waste can be effectively sintered with glass at a 10:1 (clinoptilolite to glass) ratio without the application of external pressure [9]. This is particularly feasible because clinoptilolite waste features a chemical composition similar to that of glass. However, solidifying high-melting-point sludges—such as Fe_2O_3, Cr_2O_3, and NiO—under pressureless conditions is particularly difficult when only a small amount (≈10 %) of glass is used. Further experimental findings indicate that the addition of 10 % glassy material within the 800–1000 °C range promotes the stable solidification of sludges—composed of 70 % Fe_2O_3, 18 % Cr_2O_3, and 12 % NiO—originating from metallic structures. This process is further enhanced by hot isostatic pressing treatment [10].

Although thermal durability under standard disposal conditions is not currently mandated by regulatory criteria, long-term environmental exposure—such as seasonal temperature variations or accidental thermal excursions—may still compromise the integrity of solidified waste. To address this risk, assessing material stability under thermal cycling conditions ranging from −40 °C to 60 °C (ASTM B553) is essential. This cycling range is also specified in the Korea Radioactive Waste Agency disposal acceptance criteria. The solidified waste produced in this study at temperatures exceeding several hundred degrees Celsius is expected to exhibit sufficient thermal robustness under these conditions. However, stable solidification can be complicated by the variable melting points of sludge components, especially as the proportion of high-melting-point oxides increases. Specifically, Fe_2O_3, Cr_2O_3, and NiO exhibit melting points of approximately 1596 °C, 2435 °C, and 1955 °C, respectively [11–13]. Among these, Fe_2O_3 is anticipated to be the dominant component in sludge resulting from the corrosion of stainless steel. Nonetheless, accurately determining the formation ratios of individual sludge components remains a formidable challenge. This complexity underscores the importance of evaluating whether a stable solidified waste form can be produced using 10–20 % glassy material, even when the proportion of Cr_2O_3 or NiO—both with higher melting points—is comparable to that of Fe_2O_3. Moreover, identifying the key factors contributing to the stable solidification of radioactive sludge is essential for effective waste management. In this context, the present study investigates the effect of varying B_2O_3 content on the leaching resistance of the solidified waste matrix. Additionally, it examines how the sludge-to-ferro frit ratio and heating temperature influence the leaching resistance of the solidified product.

2. Methods

2.1. Materials

Given that most metallic components used in NPPs are constructed from stainless steel, Fe_2O_3, Cr_2O_3, and NiO were selected as the primary constituents of the simulated sludge in this study [2]. These oxides are typical corrosion byproducts of stainless steel, and given their high melting points—1596 °C, 2435 °C, and 1955 °C, respectively—they serve as representative examples of sludge components for high-temperature systems. However, accurately quantifying the relative proportions of these oxides is challenging, as their formation is sensitive to specific corrosion conditions. In particular, factors such as temperature, duration of exposure to corrosive liquids, and the chemical nature of these liquids in contact with the metal can all influence sludge development [14,15]. Consequently, the composition of corrosion-derived sludge can vary depending on the conditions of tank usage and the operating environment, with the above mentioned variables directly impacting the relative formation ratios of Fe_2O_3, Cr_2O_3, and NiO. To account for this compositional variability, the sludge considered in this study was modeled based on the composition of SUS 304 stainless steel, a structural material most widely used in NPPs. Accordingly, the oxide mixture was prepared using the representative elemental proportions of Fe (70 %), Cr (18 %), and Ni (12 %) in SUS 304 [16]. Co, a corrosion product commonly formed in nuclear facilities, becomes activated through contact with the primary coolant and Co-alloy-based structures [2]. In addition to its role in corrosion, Co serves as a representative radionuclide in homogeneous radioactive waste solidification and in leachability assessments conducted in South Korea. However, owing to safety concerns and regulatory limitations associated with radiation exposure, handling radioactive substances (e.g., Co, Fe, Cr, and Ni) in powder form is not feasible at the laboratory scale. To address this limitation, Co powder was incorporated into the stainless-steel-based mixture to create a simulated sludge, with ferro frit added as an auxiliary additive, as shown in Fig. 1. Consequently, mass spectrometry instead of radiological instrumentation was employed to quantify leached elements from the simulated sludge.

Ferro frit is a glassy material commonly used as a glaze in porcelain production. To facilitate its application as a glaze, ferro fit is typically dissolved in water and coated onto porcelain surfaces, where it solidifies upon heating, thereby enhancing the durability of the final product. In this study, the leaching stability of the solidified sludge was evaluated by comparing its leachability index with established leaching stability criteria for solidified radioactive waste. As stated, mass spectrometry was employed to quantify the leached elements. To prepare the samples, a homogeneous mixture of simulated sludge powders—Fe_2O_3, Cr_2O_3, NiO, and Co—was blended with ferro frit. The chemical reagents used were Cr(III) oxide (Cr_2O_3, 98.5 % purity, SAMCHUN), Fe(III) oxide (Fe_2O_3, 93 % purity, DAEJUNG), Ni(II) oxide (NiO, 70 % Ni content, DUKSAN), and Co powder (Co, 99.5 % purity, DAEJUNG). The mixed powder was then pressed at ambient temperature to achieve densification and shaping, followed by heating to facilitate sintering. Sintering was conducted at 800, 850, 900, and 950 °C, in accordance with the softening temperature range of ferro frit (Table 1).

Previous studies have demonstrated that a mixture of 10 % ferro frit 3195 and 90 % sludge, heated between 900 and 1000 °C, produces a stable solidified product [10]. However, evaluating whether ferro frit 3195 alone possesses the specific characteristics required to serve as an effective auxiliary additive for stable solidified waste formation remains essential. If solidified sludge produced using alternative glassy materials—excluding ferro frit 3195—exhibits instability, this would suggest that a unique property of ferro frit 3195 is critical to achieving sludge stability. As indicated in Table 1, the overall composition and softening temperature (glass transition temperature) of ferro frit 3110 are comparable to those of ferro frit 3195, although differences exist in the ratios of individual components.

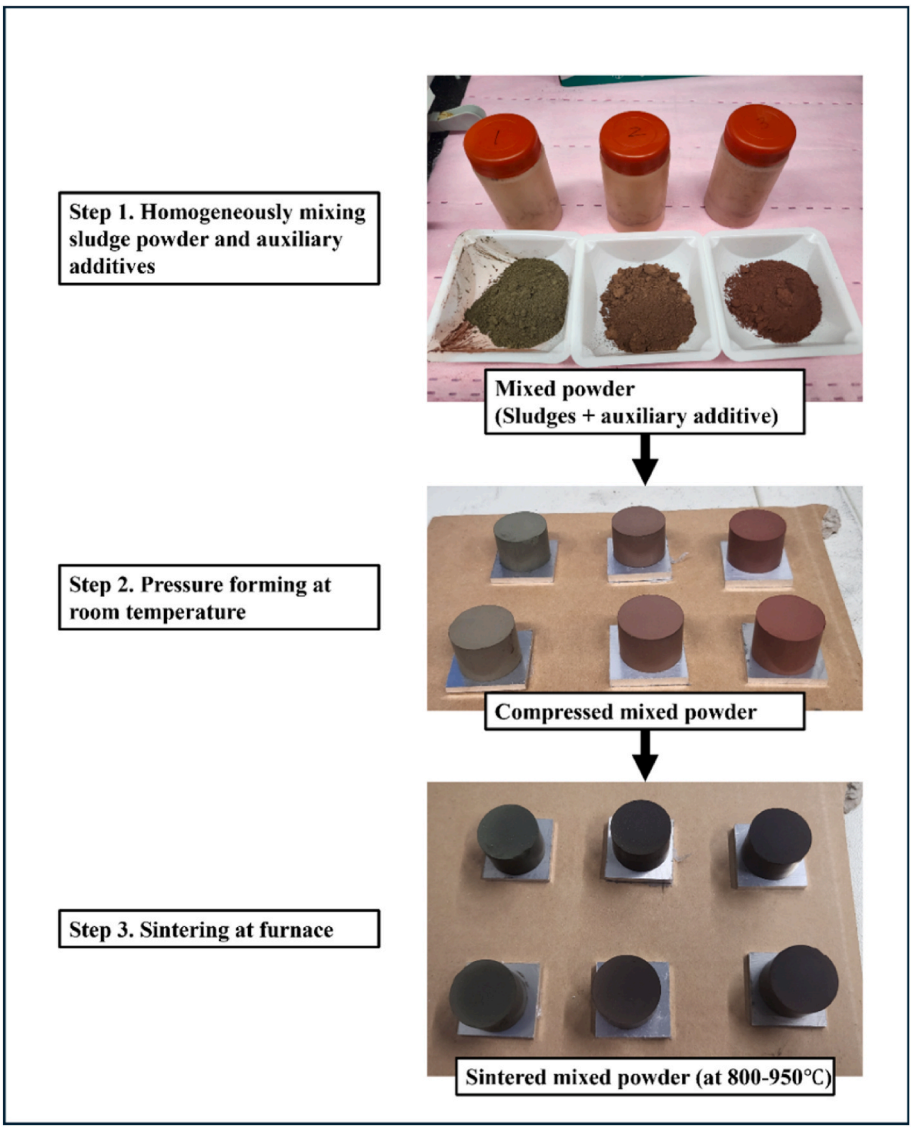

Fig. 1. Production process of solidified sludge.

Table 1
Composition and softening temperature of ferro frit 3195 and ferro frit 3110.

Component	Ferro frit 3195 (%)	Ferro frit 3110 (%)
Na_2O	5.7	15.3
K_2O	–	2.3
CaO	11.3	6.3
Al_2O_3	12.1	3.7
B_2O_3	22.4	2.6
SiO_2	48.5	69.8
Total	100	100
Softening temperature (°C)	816–927	760–927

Specifically, ferro frit 3110 contains a higher proportion of SiO_2, a fundamental component of the glass network structure. In contrast, ferro frit 3195 has a greater concentration of B_2O_3. Although B_2O_3 also contributes to glass network formation, its melting point is much lower—approximately 450 °C [17]—than that of SiO_2 (1710 °C) [18]. Thus, B_2O_3 functions as a flux, reducing the melting temperature of the glass mixture. This compound is also known to improve the chemical durability of glass. Although Na_2O and K_2O are also utilized as fluxing agents in glass production, their primary role is to decrease the viscosity of glass. Notably, Na_2O has a melting point of approximately 1132 °C—substantially higher than that of B_2O_3—whereas K_2O melts at around 350 °C. Overall, ferro frit 3110 contains more SiO_2 and less B_2O_3 than ferro frit 3195.

In parallel, ferro frit 3110 contains higher levels of Na_2O and K_2O than ferro frit 3195. In contrast, ferro frit 3195 includes greater proportions of CaO (melting point ≈ 2572 °C) and Al_2O_3 (≈2051 °C), both of which exhibit much higher melting points than those of the components of ferro frit 3110. In this study, the proportion of auxiliary additives was maintained below 20 %, which is substantially lower than the sludge content, constituting 80–90 % of the total mixture. Co powder was added at 10 wt% in all samples to ensure both detectability and homogeneity within the simulated sludge system. Although this level does not reflect the specific activity of Co-60 in actual radioactive waste, microgram-scale Co addition was not feasible owing to limitations in weighing precision and analytical sensitivity. Consequently, even with the reduced melting point of the mixed powder—comprising ferro frit and sludge— achieving full melting at 950 °C remains challenging. Under these conditions, some of the molten material serves as a binder, securing the remaining unmelted particles and allowing the solidified sludge to retain its pressurized state. This process is analogous to sintering, where powder is first compressed to minimize interparticle distance and subsequently heated. In conventional sintering, however, a

stable body is typically formed only when the temperature reaches around 80 % of the material's melting point. Given that the sludge has a melting point above 1500 °C and constitutes a greater proportion of the mixture than the auxiliary additive (ferro frit), forming a stable sintered body at 950 °C remains difficult. Nonetheless, previous studies [10] have demonstrated that stable solidification at 900–1000 °C is possible with the addition of 10 % ferro frit 3195. This is because the frit reaches its softening point, acts as an adhesive, and partially bonds with the sludge, promoting melting. Consequently, the samples containing ferro frit 3195 were designated as the control group, as indicated in Table 2. Building on the methodology adopted in previous studies, this study explored whether ferro frit 3110—which exhibits a softening temperature range similar to that of ferro frit 3195—could be used to achieve stable solidification. Furthermore, as the effectiveness of ferro frit 3195 in producing a stable solidified body was previously demonstrated [10], it was used as the control group in this investigation. The primary aim was to determine whether ferro frit 3110, which shares similar thermal and chemical characteristics with ferro frit 3195, could deliver comparable performance. Given that the most notable difference between the two frits lies in their B_2O_3 content, which is substantially lower in ferro frit 3110, additional (Group B) experiments were designed to assess the influence of B_2O_3 on solidification behavior. As indicated in Table 2, tests were conducted to confirm the capability of ferro frit 3110 to solidify sludge. Heating temperatures of 800, 850, 900, and 950 °C were selected based on the softening range of the frit. These 50 °C increments were chosen to clearly distinguish heating effects, minimizing overlap owing to potential measurement deviations. Notably, among the heating temperatures selected for Group A samples (Table 2), 800 °C falls within the softening range of ferro frit 3110 but lies near its lower boundary (760–927 °C). The midpoint of this range is approximately 843.5 °C. Further, 850 °C lies slightly above this midpoint, while 900 °C remains within the range but approaches its upper limit. In contrast, 950 °C exceeds the upper boundary of 927 °C. In parallel, increasing the ferro frit 3110 content from 10 % to 20 % requires evaluation of the leaching concentrations of key sludge constituents—Fe, Cr, Ni, and Co. Generally, increasing the proportion of the auxiliary additive improves the leaching resistance of the solidified product, thereby enhancing its overall stability. As part of the experimental design, 1–3 % of B_2O_3 was introduced as an auxiliary component. The B_2O_3/SiO_2 ratios of samples B1, B2, and B3 were approximately 0.181, 0.324, and 0.467, respectively. B_2O_3 is a vital glass-forming agent, as it contributes to the network structure and simultaneously lowers the melting point. Notably, if leaching concentrations in group A samples exceed those in the control samples, this difference may stem from the varying B_2O_3 contents of ferro frits 3195 and 3110. To further explore the independent role of B_2O_3 in solidification performance, group C was designed with B_2O_3 as the sole auxiliary additive. In this context, we had to evaluate whether stable solidification could still be achieved. Generally, increasing the proportion of a low-melting-point material helps reduce the mixture's overall melting point. Even in smaller quantities, however, materials with exceptionally low melting points can still contribute effectively to lowering the melting temperature. If group C samples demonstrate superior performance than the control group samples, B_2O_3 could serve as a practical alternative to ferro frit 3195.

After determining the optimal conditions for stable sludge solidification, the effectiveness of the same method was assessed in a scenario wherein the ratios of Fe_2O_3, Cr_2O_3, and NiO in the sludge were altered. Based on the typical composition of stainless steel, Fe_2O_3 is likely the most abundant oxide in the sludge; however, it has a lower melting point than Cr_2O_3 and NiO. As indicated in Table 3, although the proportion of high-melting-point components increases, it remains essential to verify whether stable solidification can still be achieved by adding a small amount of auxiliary additive and heating at 950 °C [10]. In particular, adjusting the ratios of Cr_2O_3 and NiO is important when the Fe_2O_3:Cr_2O_3:NiO composition is modified to 50:28:22 or 30:38:32. To confirm the effectiveness of these compositions, the leaching resistance of the resulting solidified bodies must be verified under the same processing conditions reported in previous studies [10]. Group D samples were fabricated according to the specifications listed in Table 3. To enhance the leaching stability of the solidified body, ferro frit 3195—a glassy material with a high B_2O_3/SiO_2 ratio—was incorporated as the auxiliary additive. As indicated in Table 3, when the sludge component ratio (Fe_2O_3:Cr_2O_3:NiO) was varied from 70:18:12 to 50:28:22 and then to 30:38:32, we verified whether stable solidification could still be achieved using 10 % ferro frit 3195 and heating at 950 °C. In this context, prior to evaluating leaching resistance, the surface durability of the solidified body must be confirmed. If sludge components are dislodged by light rubbing, the material can be considered unstable.

Table 2
Solidification conditions using ferro frit 3110 and B_2O_3 as auxiliary additives.

Group	Sample	Simulated sludge composition	Auxiliary additive	Ratio (frit: sludge)	Heating temperature (°C)
A	A1	(Fe_2O_3:Cr_2O_3:NiO = 70:18:12) + Co powder	Ferro frit 3110	10:90	800
	A2			15:85	
	A3			20:80	
	A4			10:90	850
	A5			15:85	
	A6			20:80	
	A7			10:90	900
	A8			15:85	
	A9			20:80	
	A10			10:90	950
	A11			15:85	
	A12			20:80	
Control group	CG		Ferro frit 3195	10:90	950
Group	**Sample**	**Simulated sludge composition**	**Auxiliary additive**	**Ratio (frit: B_2O_3: sludge)**	**Heating temperature (°C)**
B	B1	(Fe_2O_3:Cr_2O_3:NiO = 70:18:12) + Co powder	Ferro frit 3110 +B_2O_3	10:1:89	950
	B2		Ferro frit 3110 +B_2O_3	10:2:88	950
	B3		Ferro frit 3110 +B_2O_3	10:3:87	950
Group	**Sample**	**Simulated sludge composition**	**Auxiliary additive**	**Ratio (B_2O_3: sludge)**	**Heating temperature (°C)**
C	C1	(Fe_2O_3:Cr_2O_3:NiO = 70:18:12) + Co powder	B_2O_3	10:90	950
	C2		B_2O_3	15:85	950

Table 3
Solidification conditions using an optimal auxiliary additive (ferro frit 3195).

Group	Sample	Simulated sludge composition	Auxiliary additive	Ratio (frit: sludge)	Heating temperature (°C)
D	**D1**	(Fe_2O_3:Cr_2O_3:NiO = 50:28:22) + Co powder	Ferro frit 3195	10:90	950 → 970 → … → 1030 → 1050
	D2	(Fe_2O_3:Cr_2O_3:NiO = 30:38:32) + Co powder	Ferro frit 3195	10:90	

2.2. Leaching stability evaluation

Evaluating leaching resistance is a critical aspect of ensuring the stable solidification of radioactive sludge. If the solidified mass lacks stability, its resistance to leaching may be substantially compromised. This condition presents a serious environmental risk, as radionuclides in the waste can dissolve into groundwater and lead to contamination when groundwater infiltrates the disposal site. Therefore, improving leaching resistance through stable sludge solidification is essential. In Korea, the leaching stability of solidified bodies is assessed using leachability tests based on the American National Standard (ANS)-16.1–2019 [19]. In accordance with this standard, the solidified samples were fabricated in cylindrical shapes, with length-to-diameter ratios between 0.2 and 5. Following the leaching tests, the leachability index (L) and effective diffusivity (D) were calculated in alignment with the American National Standard for the Measurement of the Leachability of Solidified Low-Level Radioactive Wastes by a Short-Term Test Procedure (ANSI/ANS-16.1-2019) [19]. According to Korean disposal regulations, a solidified body composed of homogeneous radioactive waste is eligible for disposal only if the leachability index is at least six. In this study, the leachability index was evaluated over a 5-day period using deionized (DI) water as the leachate. Over the study period, the leachate was collected every 24 h (±0.5 h), and the solidified sample was then re-immersed in fresh DI water. To assess the concentrations of leached elements and to compute the L and D values, leachate samples were collected in total. The concentrations of the sludge components—specifically Co, Fe, Cr, and Ni—were analyzed using inductively coupled plasma–mass spectrometry (ICP–MS). Given that extremely low concentrations of leached components were observed across all samples, five-day average values were used to calculate D, aiming to reduce analytical time and cost. However, this approach may be unsuitable when leached concentrations are substantially higher, as it can underestimate variations in the early leaching stages. Following the 5-day leachability evaluation, the parameter D, expressed in square centimeters per second, was compared against the reference value β (1.0 cm^2/s). The L value was then calculated as the ratio of D to β. In accordance with ANS-16.1-2019 guidelines, L and D were determined using the formulas provided in Eqs. (1) and (2).

$$\mathrm{D} = \frac{\pi}{4} \times \left(\frac{\sum_{i=1}^{4} a_i}{A_0} \times \frac{V}{S} \right)^2 \times \frac{1}{\sum_{i=1}^{4} t}, \tag{1}$$

$$\mathrm{L} = \log\left(\beta D_i\right), \tag{2}$$

where D denotes the effective diffusivity (cm^2/s); a_i represents the leached mass of the target material (Co, Fe, Cr, or Ni) in the leachate during the ith leaching interval (g); A_0 denotes the initial total mass of the target material (Co, Fe, Cr, or Ni) in the solidified body (g); V/S represents the volume-to-surface-area ratio, defined as the volume of leachate (cm^3) divided by the surface area of the solidified body (cm^2) and set to 10 cm (as recommended in ANS-16.1-2019); t represents leaching time per test interval, defined as the leachate replacement period (24 ± 0.5 h, ANS-16.1-2019 recommendation); β denotes the reference constant for diffusivity (1.0 cm^2/s; ANS-16.1-2019 recommendation), and L is the leachability index (unitless).

If the solidified body exhibits leaching instability within the first 24 h—or if the leachate displays visible signs of contamination—it can be considered unstable before completing the full 5-day leachability test. Based on this criterion, the leaching resistance of samples from groups A, B, and C was assessed. The concentrations of Fe, Ni, Cr, and Co leached during the first 24 h were compared with those in the control group to determine the relative stability of each sample. The optimal auxiliary additive and solidification conditions were identified based on the experimental results corresponding to the solidification conditions listed in Table 2. These optimal parameters were then used to evaluate the leachability indices of the samples presented in Table 3.

2.3. X-ray photoelectron spectroscopy (XPS) analysis

The microstructure of the solidified sludge was examined using XPS. While scanning electron microscopy with energy dispersive X-ray spectroscopy can provide information on elemental composition ratios, it cannot reveal the chemical bonding states of the elements. Likewise, X-ray diffraction does not support quantitative component analysis. Therefore, XPS was deemed the most appropriate technique for microstructural analysis in this study. As indicated in Table 1, the compositions and softening temperature ranges of ferro frits 3195 and 3110 suggest that the samples in Group A and the control group (Table 2) are likely to possess similar chemical compositions. Although ferro frit—a glassy material—was incorporated into the sludge solidification process, this method differs from conventional vitrification, which entails melting a mixture of glass and sludge. In the present study, ferro frit served solely as an auxiliary additive rather than as a primary matrix component.

Given that the melting point of the sludge components exceeds 1500 °C, most of the sludge is expected to remain in a solid state during processing. In conventional sintering, materials are typically heated to approximately 80 % of their melting point and compressed to promote solidification. While this study was based on the fundamental principles of sintering, the processing temperature used was considerably lower than the melting point of the mixture, which comprised 90 % sludge and 10 % ferro frit.

Within the softening temperature range, ferro frit softens and acts as an adhesive, allowing a small amount to bind with and partially melt the surrounding sludge, unlike in conventional sintering. Ferro frits 3195 and 3110 exhibit notably similar softening temperatures and chemical compositions. Additionally, both the A1–12 samples prepared using ferro frit 3110 and the control group samples prepared using ferro frit 3195 share the same sludge composition ratio (Fe_2O_3:Cr_2O_3:NiO = 70:18:12). Consequently, similar XPS spectra are anticipated, which may complicate efforts to identify the factors responsible for differences in sludge leaching behavior between the two sample sets. If discrepancies do arise, it would be essential to investigate the specific characteristics of each component in the ferro frits.

3. Results and discussion

3.1. Leached concentration and leachability index

The experimental findings presented in Table 2 are summarized in Table 4. In several leachate samples (A1, A2, A10, A11), Fe was not detected, indicating that the signal associated with leached Fe was below the background equivalent concentration limit of the ICP–MS instrument. However, when Fe was detected in other samples, its concentration was considerably lower than 600 mg/L, suggesting minimal leaching. Notably, for the leachability index of Fe in solidified sludge to exceed six, the leached Fe concentration must remain below approximately 600 mg/L. In sample A3, the Fe concentration in the leachate was 0.012 ± (8.82×10^{-5}) μg/L, while in A12 it was 0.054 ± (4.07×10^{-3}) μg/L. Thus, both concentrations remained below 0.1 μg/L. However, establishing the statistical significance of the observed difference of 0.042 μg/L is challenging. Excluding A3, A12, and CG, all other samples exhibited Fe concentrations exceeding 1 μg/L. Nevertheless, when compared with the 600 mg/L threshold, even the highest of these values was more than 30,000 times lower (e.g., 20 μg/L vs. 600 mg/L) and thus not considered elevated. In Group B, the Fe concentrations were recorded as 2.12 ± (3.96×10^{-2}), 1.48 ± (3.96×10^{-2}), and 3.94 ± (4.21×10^{-1}) μg/L for B1, B2, and B3, respectively—all of which were substantially below the 600 mg/L limit. For Ni, all samples recorded leached

Table 4
Leached concentrations of sludge components after 24 h.

Group	Sample	Concentrations of leached sludge components			
		Fe (μg/L)	Cr (mg/L)	Ni (μg/L)	Co (μg/L)
A	A1	–	$28.6 \pm (4.01 \times 10^{-1})$	$0.488 \pm (1.14 \times 10^{-2})$	$0.702 \pm (1.27 \times 10^{-2})$
	A2	–	$45.1 \pm (4.96 \times 10^{-1})$	$0.279 \pm (2.30 \times 10^{-3})$	$0.632 \pm (1.63 \times 10^{-3})$
	A3	$0.012 \pm (8.82 \times 10^{-5})$	$33.8 \pm (1.69 \times 10^{-1})$	$0.193 \pm (1.76 \times 10^{-3})$	$0.744 \pm (3.30 \times 10^{-3})$
	A4	$11.4 \pm (2.09 \times 10^{-1})$	$81.2 \pm (4.87 \times 10^{-1})$	$1.59 \pm (5.02 \times 10^{-2})$	$1.43 \pm (5.14 \times 10^{-2})$
	A5	$13.5 \pm (1.37 \times 10^{-1})$	$146 \pm (4.40 \times 10^{-1})$	$3.54 \pm (1.98 \times 10^{-2})$	$3.54 \pm (4.10 \times 10^{-2})$
	A6	$9.96 \pm (1.07 \times 10^{-1})$	$26.0 \pm (2.34 \times 10^{-1})$	$0.641 \pm (1.95 \times 10^{-2})$	$1.03 \pm (1.20 \times 10^{-2})$
	A7	$8.48 \pm (9.61 \times 10^{-2})$	$35.9 \pm (1.43 \times 10^{-1})$	$0.960 \pm (2.30 \times 10^{-2})$	$0.261 \pm (6.87 \times 10^{-3})$
	A8	$13.3 \pm (1.54 \times 10^{-1})$	$23.2 \pm (9.28 \times 10^{-2})$	$0.563 \pm (1.00 \times 10^{-3})$	$0.317 \pm (4.31 \times 10^{-3})$
	A9	$14.7 \pm (2.15 \times 10^{-1})$	$69.8 \pm (2.79 \times 10^{-1})$	$0.967 \pm (1.54 \times 10^{-2})$	$1.06 \pm (1.93 \times 10^{-2})$
	A10	–	$23.8 \pm (2.62 \times 10^{-1})$	$0.200 \pm (7.38 \times 10^{-3})$	$0.220 \pm (7.54 \times 10^{-3})$
	A11	–	$4.59 \pm (1.88 \times 10^{-1})$	$0.107 \pm (2.67 \times 10^{-3})$	$0.438 \pm (6.75 \times 10^{-3})$
	A12	$0.054 \pm (4.07 \times 10^{-3})$	$1.24 \pm (2.46 \times 10^{-1})$	$0.079 \pm (5.78 \times 10^{-3})$	$0.645 \pm (1.49 \times 10^{-2})$
Control group	CG	$0.038 \pm (3.32 \times 10^{-3})$	$0.018 \pm (3.60 \times 10^{-4})$	$0.448 \pm (1.06 \times 10^{-2})$	$1.198 \pm (2.81 \times 10^{-2})$
B	B1	$2.12 \pm (3.96 \times 10^{-2})$	$5.37 \pm (1.04 \times 10^{0})$	$0.058 \pm (1.05 \times 10^{-2})$	$0.306 \pm (7.94 \times 10^{-3})$
	B2	$1.48 \pm (3.96 \times 10^{-2})$	$2.06 \pm (2.68 \times 10^{-2})$	$0.211 \pm (1.76 \times 10^{-2})$	$0.374 \pm (1.47 \times 10^{-2})$
	B3	$3.94 \pm (4.21 \times 10^{-1})$	$0.431 \pm (1.29 \times 10^{-3})$	$0.560 \pm (4.43 \times 10^{-3})$	$0.860 \pm (2.66 \times 10^{-2})$
C (Damaged samples)	C1	–	–	–	–
	C2	–	–	–	–

concentrations below 1 μg/L, with the exception of A4 and A5.

For the leachability index to exceed six, the leached concentration of Ni must remain below approximately 100 mg/L; however, all recorded values (Table 4) were considerably lower than this critical threshold. For Co, a leachability index greater than six requires the leached concentration to remain below approximately 80 mg/L. Although the Co concentrations in samples A4, A5, A6, and A9 and the control group were slightly higher than 1 μg/L, this level remains negligible in comparison to 80 mg/L and cannot be considered abnormal. In contrast, the leached concentrations of Cr were notably higher than those of the other sludge components—Fe, Ni, and Co. This is outlined in Table 4, where the leached Cr concentrations are specified in milligrams per liter. In the control group sample, the Cr concentration was approximately 18 μg/L (or 0.018 mg/L).

Compared to the leached concentrations of the other sludge components, the Cr concentration of 18 μg/L (or 0.018 mg/L) is relatively high. However, this value remains well below the threshold required to exceed a leachability index of six, which corresponds to a leached Cr concentration of approximately 200 mg/L. Specifically, 18 μg/L is less than 20 μg/L, representing only 1/10,000 of the 200 mg/L benchmark. This behavior is likely attributed to the fact that Cr_2O_3 exhibits the highest melting point among the sludge oxides. Furthermore, with the exception of the control group sample prepared using ferro frit 3195, all samples demonstrated markedly higher leached Cr concentrations than those of the other sludge components (Fe, Ni, and Co). This trend suggests that Cr_2O_3 was not effectively immobilized within the solidified matrices of the Group A samples prepared using ferro frit 3110, unlike the case for the control group sample incorporating ferro frit 3195. In samples A1–A3, which were heat-treated at 800 °C, the leached Cr concentrations were $28.6 \pm (4.01 \times 10^{-1})$, $45.1 \pm (4.96 \times 10^{-1})$, $33.8 \pm (1.69 \times 10^{-1})$ μg/L, respectively, corresponding to increasing ferro frit 3110 contents from 10 % to 20 %. Despite the increased ratio of ferro frit 3110, the concentration of leached Cr remained largely unchanged, indicating that increasing the amount of ferro frit 3110 at 800 °C does not improve Cr leaching resistance. This trend also persisted at heating temperatures of 850 °C and 900 °C. Although the 800–900 °C range falls within the softening temperature range of ferro frit 3110 (760–927 °C), it appears insufficient for enhancing the leaching resistance of Cr_2O_3, which has the highest melting point among the sludge components. In a comparative analysis of samples with identical ferro frit 3110 ratios, sample A10—heated at 950 °C—exhibited a lower leached Cr concentration than samples A1, A4, and A7, which were heated at temperatures between 800 °C and 900 °C. A similar pattern was observed for samples A11 and A12, suggesting that Cr leaching stability within the solidified matrix improves when the heating temperature exceeds the upper limit of the softening range.

In samples A10–A12 treated at 950 °C, increasing the ratio of ferro frit 3110 led to improved Cr leaching stability. Moreover, replacing ferro frit 3195 with ferro frit 3110 as the auxiliary additive did not adversely affect the leaching resistance of Fe, Ni, or Co when compared to the control sample. Within group A, although Cr leaching was less stable than that in the control sample containing ferro frit 3195, a higher ratio of ferro frit 3110 helped enhance Cr resistance when the heating temperature slightly exceeded the softening point. However, in the case of Cr, the leached concentration in sample A12 exceeded that in the control group sample, despite the additive ratio of ferro frit 3110 being 20 %—notably higher than the 10 % ratio used for ferro frit 3195 in the control group. This unexpected result may be attributed to specific components within ferro frit 3195. In glassy materials such as ferro frit, SiO_2 and B_2O_3 are essential for forming the glass network structure. However, the solidified bodies fabricated in this study differ from conventional vitrified products. Considering that the additive ratio of glassy material ranges only from 10 % to 20 %—substantially lower than the sludge content—the process follows principles similar to sintering. Sintering occurs when a solid body is heated to approximately 80 % of the melting point of its primary components. In this study, the dominant constituent of the solidified material is sludge, accounting for 80–90 % of the total composition. Therefore, the solidification mechanism observed can be interpreted as the immobilization of sludge facilitated by molten ferro frit, combined with a sintering-like process involving both pressurization and heating.

Although ferro frits 3110 and 3195 have comparable softening

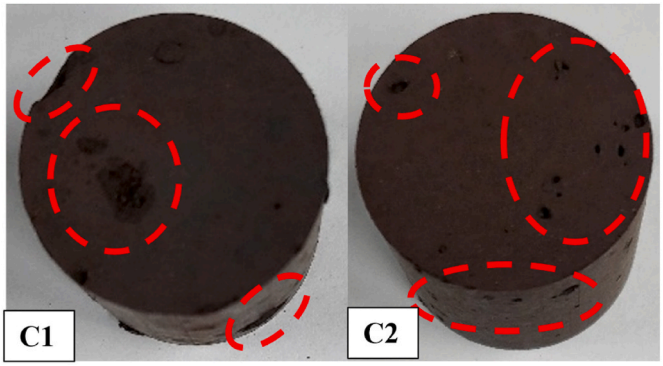

Fig. 2. Group C samples following heating at 950 °C.

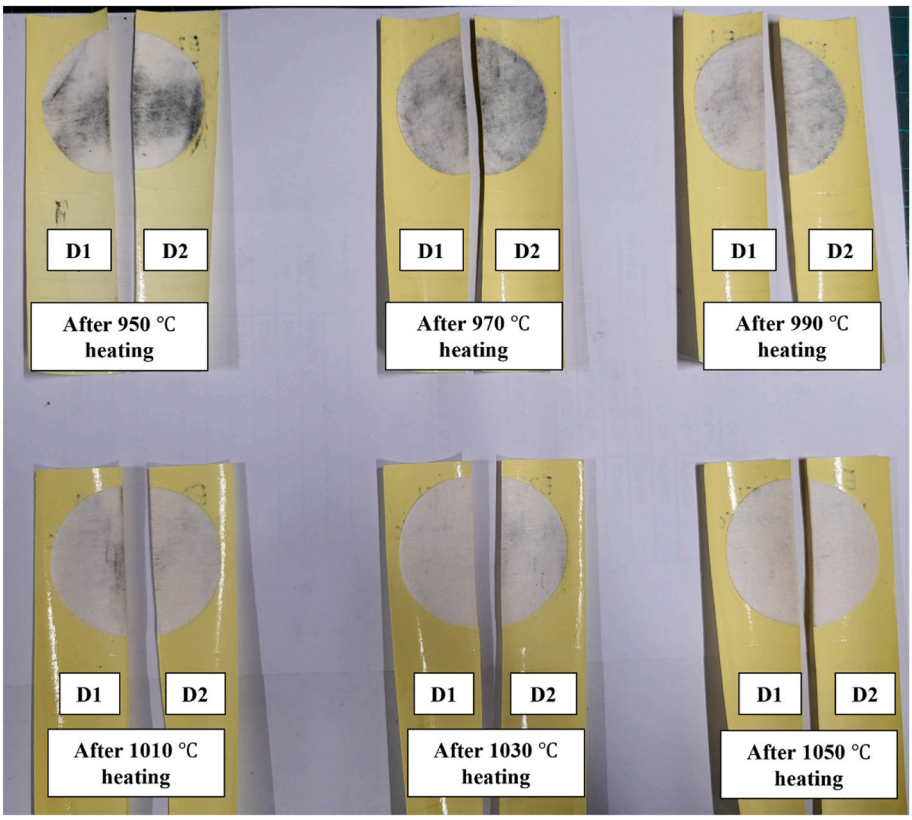

Fig. 3. Wear resistance of group D samples as a function of heating temperature (950–1050 °C).

Table 5
Average mass of sludge deposited on smear paper after heating at 1010–1050 °C (group D).

Sample	Temperature (°C)	Average sludge mass on smear paper (μg)			
		Fe	Cr	Ni	Co
D1	1010	28.4	15.3	42.3	15.2
D2					
D1	1030	25.6	13.6	47.1	16.6
D2					
D1	1050	13.6	7.01	17.2	6.46
D2					

temperature ranges, as indicated in Table 1, ferro frit 3195 exhibits a markedly higher B_2O_3/SiO_2 ratio of approximately 0.462 compared to ferro frit 3110 (0.037). This disparity in the B_2O_3/SiO_2 ratio may be a critical factor influencing the distinct chemical behaviors and leaching characteristics observed between the two ferro frits. B_2O_3 not only contributes to the formation of the glass network structure but also functions as a flux that lowers the melting point of the mixture. Thus, the differences in leached Cr concentrations between samples containing ferro frits 3195 and 3110 can be attributed to their differing B_2O_3/SiO_2 ratios, despite their similar softening temperature ranges. The observed improvement in Cr leaching resistance with increasing B_2O_3 content—particularly in sample B3—can be structurally interpreted based on the role of boron in modifying the glass network [20]. B_2O_3 enhances the degree of polymerization in the glass structure and reduces the number of non-bridging oxygen atoms, resulting in a denser and more interconnected network. This structural transformation limits the mobility of ionic species and restricts the chemical pathways available for aqueous infiltration. Consequently, Cr species—especially Cr^{3+}— are more effectively immobilized within the matrix, thereby improving leaching resistance under disposal conditions. In Group B, a positive correlation was observed between the increase in B_2O_3 content (1–3 %) and the enhancement of Cr leaching resistance across the samples. Specifically, the B_2O_3/SiO_2 ratios of samples B1, B2, and B3 were 0.181, 0.324, and 0.467, respectively. A particularly noteworthy comparison can be drawn between samples A12 and B3: In sample A12, the auxiliary additive (ferro frit 3110) accounted for 20 % of the composition, while in sample B3, the combined auxiliary additive (ferro frit 3110 and B_2O_3) comprised only 13 %. The leached Cr concentration in sample B3 was measured at 0.431 g/L ± (1.29×10^{-3}) μg/L, which was substantially lower than the value of 1.24 g/L ± (2.46×10^{-1}) μg/L detected in sample A12. When the heating temperature and the type of auxiliary additive were fixed at 950 °C and ferro frit 3110, respectively, increasing the proportion of the auxiliary additive led to improved Cr leaching resistance in the solidified body. Nonetheless, at a constant heating temperature of 950 °C, the type of auxiliary additive had a greater impact on the stability of the solidified body than the additive ratio itself.

Table 6
Leachability index of the solidified body after heating at 1050 °C (group D).

Group	Sample	Leachability index			
		Fe	Cr	Ni	Co
D	D1	15.0 ± 0.207	15.3 ± 0.332	14.0 ± 0.167	14.2 ± 0.208
	D2	13.2 ± 0.208	13.6 ± 0.333	15.4 ± 0.208	15.5 ± 0.209

Table 7
Highest binding energy peaks identified in XPS wide-scan analysis.

	Sample					
Temperature (°C)	800			850		
Spectral line	**A1**	**A2**	**A3**	**A4**	**A5**	**A6**
	Highest peak binding energy (eV)					
Na1s	1071.3	1071.0	1070.1	1070.7	1071.2	1070.8
B1s	–	–	–	–	–	–
Fe2$p_{3/2}$	711	710.2	709.6	710.4	710.3	710.9
Cr2$p_{3/2}$	576.2	576.6	575.2	575.8	576.4	575.8
Co2$p_{3/2}$	780.1	780.7	779.1	780.0	780.2	779.8
Si2p	102.5	102.2	102.0	101.9	102.2	102.0
Ca2$p_{1/2}$	347.5	–	346.8	–	–	–
Ni2$p_{3/2}$	854.6	855	853.4	854.3	854.5	854.3
Al2p	–	–	–	–	–	–
Spectral line	**Chemical formula of sludge components in the solidified body**					
Na1s	Na_2O	Na_2O	Na_2O	Na_2O	Na_2O	Na_2O
B1s	–	–	–	–	–	–
Fe2$p_{3/2}$	Fe_2O_3	Fe_2O_3	Fe_2O_3	Fe_2O_3	Fe_2O_3	Fe_2O_3
Cr2$p_{3/2}$	Cr_2O_3	Cr_2O_3	Cr_2O_3	Cr_2O_3	Cr_2O_3	Cr_2O_3
Co2$p_{3/2}$	Co_2O_3, Co_3O_4	Co_2O_3, Co_3O_4	Co_2O_3, Co_3O_4	Co_2O_3, Co_3O_4	Co_2O_3, Co_3O_4	Co_2O_3, Co_3O_4
Si2p	SiO_2, Metal SiO_4 $((SiO_4)^{4-})$	SiO_2, Metal SiO_4 $((SiO_4)^{4-})$	SiO_2, Metal SiO_4 $((SiO_4)^{4-})$	SiO_2, Metal SiO_4 $((SiO_4)^{4-})$	SiO_2, Metal SiO_4 $((SiO_4)^{4-})$	SiO_2, Metal SiO_4 $((SiO_4)^{4-})$
Ca2$p_{1/2}$	CaO	–	CaO	–	–	–
Ni2$p_{3/2}$	NiO	NiO	NiO	NiO	NiO	NiO
Al2p	–	–	–	–	–	–

Table 8
Highest binding energy peaks identified in XPS wide-scan analysis.

	Sample						
Temperature (°C)	900			950			
Spectral line	**A7**	**A8**	**A9**	**A10**	**A11**	**A12**	**CG**
	Highest peak binding energy (eV)						
Na1s	1071.0	1071.0	1071.0	1071.1	1071.8	1071.4	1071.4
B1s	–	–	–	–	–	–	191.1
Fe2$p_{3/2}$	710.2	710.6	710.5	710.2	711.1	710.9	710.5
Cr2$p_{3/2}$	576.1	576.1	578.9	575.2	575.9	576.2	575.9
Co2$p_{3/2}$	779.6	780.4	780.6	780.2	780.2	780.9	780
Si2p	102.1	102.0	102.0	101.9	102.1	102.4	102.3
Ca2$p_{1/2}$	–	–	–	346.6	346.6	347.1	347.0
Ni2$p_{3/2}$	854.3	854.8	854.0	854.3	854.5	854.6	854.5
Al2p	–	–	–	–	–	74.4	74.6
Spectral line	**Chemical formula of sludge components in the solidified body**						
Na1s	Na_2O	Na_2O	Na_2O	Na_2O	Na_2O	Na_2O	Na_2O
B1s	–	–	–	–	–	–	B_2O_3, Metal boride
Fe2$p_{3/2}$	Fe_2O_3	Fe_2O_3	Fe_2O_3	Fe_2O_3	Fe_2O_3	Fe_2O_3	Fe_2O_3
Cr2$p_{3/2}$	Cr_2O_3	Cr_2O_3	Cr_2O_3	Cr_2O_3	Cr_2O_3	Cr_2O_3	Cr_2O_3
Co2$p_{3/2}$	CoO, Co_2O_3, Co_3O_4	CoO, Co_2O_3, Co_3O_4	CoO, Co_2O_3, Co_3O_4	CoO, Co_2O_3, Co_3O_4	CoO, Co_2O_3, Co_3O_4	CoO, Co_2O_3, Co_3O_4	CoO, Co_2O_3, Co_3O_4
Si2p	SiO_2, Metal SiO_4 $((SiO_4)^{4-})$	SiO_2, Metal SiO_4 $((SiO_4)^{4-})$	SiO_2, Metal SiO_4 $((SiO_4)^{4-})$	SiO_2, Metal SiO_4 $((SiO_4)^{4-})$	SiO_2, Metal SiO_4 $((SiO_4)^{4-})$	SiO_2, Metal SiO_4 $((SiO_4)^{4-})$	SiO_2, Metal SiO_4 $((SiO_4)^{4-})$
Ca2$p_{1/2}$	–	–	–	CaO	CaO	CaO	CaO
Ni2$p_{3/2}$	NiO	NiO	NiO	NiO	NiO	NiO	NiO
Al2p	–	–	–	–	–	Al_2O_3	Al_2O_3

As illustrated in Fig. 2, the samples in Group C—which were prepared using B_2O_3 as the sole auxiliary additive—were unsuitable for forming a stable solidified body. This outcome can be attributed to the considerable difference in melting points between B_2O_3 and the sludge components. In Group C, the heating temperature of 950 °C exceeded the melting point of B_2O_3 (450 °C) but remained below the melting points of the sludge constituents. Lowering the heating temperature to better match the melting point of B_2O_3 would hinder the complex interactions between sintering and B_2O_3 melting. Conversely, increasing the temperature substantially above the melting point of B_2O_3 would lead to excessive melting and elevated fluidity. Consequently, the highly fluid, low-viscosity molten B_2O_3 could leak from the solidified body, compromising its structural integrity, as depicted in Fig. 2.

Furthermore, although the heating temperatures of 800 °C, 850 °C, and 900 °C fall within the softening temperature range of ferro frit 3110, they did not improve the leaching resistance of Cr in the solidified body, even with an increased ratio of ferro frit 3110. This outcome suggests that, within this temperature range, heating temperature has a stronger effect on leaching resistance than the additive ratio. At a constant temperature of 950 °C, a higher ratio of ferro frit 3110 corresponded to reduced leached Cr concentrations. However, when the additive ratio of ferro frit 3110 was fixed at 10 % and the sintering temperature was varied from 800 °C to 950 °C, no notable difference was observed in Cr leaching between samples A1 and A10. This indicates that simply increasing the heating temperature does not enhance Cr leaching resistance when the additive ratio remains below 15 %. The key factor

for achieving a stable solidified structure appears to be the incorporation of an auxiliary additive with a high B_2O_3/SiO_2 ratio. Although the total proportion of auxiliary additive was kept below 20 %, the addition of 3 % B_2O_3 to the 10 % ferro frit 3110 markedly improved resistance to Cr leaching, as presented in Table 4.

Moreover, Fig. 3 illustrates that some sludge components were transferred to the smear paper when samples D1 and D2—both heated at 950 °C—were rubbed. Increasing the heating temperature in 20 °C increments up to 1050 °C resulted in a noticeable suppression of this contamination phenomenon, particularly beyond 1010 °C. To quantify this effect, the mass (micrograms) of sludge components deposited on the smear paper after heating at 1010 °C, 1030 °C, and 1050 °C was analyzed using inductively coupled plasma optical emission spectrometry. The results, summarized in Table 5, indicate that the average deposited masses of Fe, Cr, Ni, and Co were lowest after heating at 1050 °C—measured at 13.6, 7.01, 17.2, and 6.46 μg, respectively. Human error is an inherent risk in experimental procedures, particularly during the manual handling of smear paper and solidified sludge, both of which can notably affect the amount of sludge detected on the smear paper. Therefore, the values presented in Table 5 should not be interpreted as absolute metrics. Nonetheless, visual inspection revealed a clear reduction in sludge contamination on the smear paper beginning at 1010 °C. If melting and structural collapse of the solidified sludge did not occur with further increases in temperature, a conservative assessment revealed that 1050 °C was the optimal temperature for the process. Accordingly, by increasing the proportions of NiO and Cr_2O_3—sludge components with relatively high melting points—the optimal temperature for forming a stable solidified mass was consequently adjusted to 1050 °C.

The leachability index of the solidified body produced under these optimal conditions (10 % ferro frit 3195 at 1050 °C) was evaluated, and the results are presented in Table 6. Notably, the leachability indices for the group D samples exceeded the threshold value of six—the accepted criterion for the disposal of solidified radioactive waste in Korea—by approximately 7–9 units. This increase corresponds to a substantial reduction in effective diffusivity, estimated to fall within the range of 10^{-9} to 10^{-7}, as indicated in Eqs. (1) and (2). Notably, this study utilized idealized, dried simulated sludge with simplified oxide compositions. In actual radioactive waste, the presence of residual moisture, heterogeneous particle sizes, and chemically diverse species may influence thermal behavior, gas evolution, and solidification performance. Although these factors were not directly examined in this study, they represent critical considerations for future research to assess the applicability of this process under real-world conditions.

3.2. XPS results

In this study, because the sludge components were not melted and vitrified, the formation of chemical compounds between these components was not expected. Our XPS analysis confirmed that most of the oxides—both from the sludge and the ferro frit—remained in their original states. Notably, the compositions of ferro frit 3195 and ferro frit 3110 are nearly identical, with only slight differences in the ratios of specific components. Moreover, both frits exhibit similar sludge compositions and softening temperature ranges. As summarized in Tables 7 and 8, XPS wide-scan analysis revealed that the B peak appeared only in the control group sample, while the Al peak appeared only in A12 and control group samples. Given the relatively low concentrations of Al_2O_3 and B_2O_3 in Ferro Frit 3110–3.7 % and 2.6 %, respectively—the absence of Al and B peaks in the other samples can be reasonably explained. The absence of the Ca peak in sample A2 does not indicate that calcium is entirely absent, as it was detected in other samples, including the control group. Similarly, the minimal presence of aluminum accounts for the absence of the Al peak in all samples except A12 and the control group. The sludge components—Fe, Cr, Ni, and Co—which constitute a substantial portion of the solidified body, along with Si, Ca, and Na, which are more abundant in the ferro frit, exhibited detectable peaks in all samples.

As the melting points of the sludge components are substantially higher than the softening temperatures of the ferro frit, most of the sludge remains in its original oxide state. Within the solidified mass, the volume of sludge far exceeds that of the ferro frit. Consequently, the primary metallic components—Fe, Cr, and Ni—are predominantly detected in their original oxidation states, namely Fe_2O_3, Cr_2O_3, and NiO. In contrast, Co undergoes oxidation during the heating process, resulting in the formation of Co_2O_3 and Co_3O_4. Notably, Co_3O_4 can decompose into CoO at approximately 900 °C, as reported in Ref. [21]. Although the reverse reaction, converting CoO back into Co_3O_4, can also occur, the rate of decomposition from Co_3O_4 to CoO is considerably faster than the reverse process, as observed in Ref. [22].

In all examined samples, with the exception of A1–A9—which were heated at temperatures ranging from 800 to 900 °C—CoO was consistently observed. From a microscopic perspective, certain regions within the solidified mass may exhibit a relatively higher concentration of ferro frit compared to that of sludge. Additionally, some areas may have partially melted into a mixture of sludge and ferro frit, resembling a vitrification process. This interaction facilitates bonding between the metal and $(SiO_4)^{4-}$ ions, leading to the formation of a glassy matrix and the possible generation of boron metal oxides, as presented in Tables 7 and 8 However, given the presence of multiple oxide types in the solidified body, accurately identifying the specific chemical formula of the resulting metal silicates based on $(SiO4)^{4-}$ and boron metal oxides remains challenging. The solidified sludge produced using ferro frit 3195 contains substantial amounts of SiO_2 and B_2O_3, which are believed to effectively stabilize Fe, Co, and Ni—similar to the stabilization effects attributed to the high SiO_2 content of ferro frit 3110. Nevertheless, the B_2O_3 concentration in ferro frit 3110, which plays a critical role in lowering the melting point and promoting glass network formation, is notably lower than that in ferro frit 3195. This disparity raises concerns regarding the stabilization of Cr, which has the highest melting point among the sludge constituents.

4. Conclusions

In this study, we investigated the stabilization of high-melting-point radioactive sludge oxides through a sintering-based solidification process using ferro frit as a curing agent. Leaching resistance was evaluated for four target elements—Fe, Cr, Ni, and Co. Moreover, the effects of auxiliary additive type, additive ratio, and sintering temperature were systematically examined. Among the evaluated additives, ferro frit 3195 proved to be the most effective. Although the softening temperature ranges of both ferro frits 3110 and 3195 were nearly identical, differences in the B_2O_3/SiO_2 ratio within the glass phase had a notable impact on leaching stability, particularly for high-melting-point sludge components such as Cr_2O_3. A heating temperature above 950 °C was identified as a key factor contributing to the leaching resistance of high-melting-point sludge oxides such as Cr_2O_3. Among the four analyzed sludge constituents, Fe, Ni, and Co consistently demonstrated excellent leaching resistance across all solidification conditions. Co, in particular, is a critically regulated nuclide in radioactive waste disposal owing to its widespread presence in structural alloys used in nuclear reactors. Although Co exhibits a high melting point in its alloyed form, it typically exists as CoO in sludge formed as a result of corrosion and aqueous waste processes. This oxide form is suitable for immobilization via sintering. In all samples, Co concentrations in the leachate remained at the micrograms per liter level, indicating that the proposed method is sufficiently robust for Co stabilization. In contrast, Cr exhibited considerably higher leached concentrations—on the order of milligrams per liter—under similar thermal and compositional conditions. This highlights the need for further optimization targeting Cr_2O_3, particularly through the use of B_2O_3-rich glass matrices and elevated sintering temperatures. The relatively higher leachability of Cr, especially under lower sintering

temperatures or reduced B_2O_3 content, necessitates more intensive stabilization measures. The incremental increase in the ratio of auxiliary additive had a negligible effect on Cr leaching concentrations when the heating temperature remained below 950 °C, indicating that additive ratio was not a primary determining factor under these conditions. In contrast, the presence of flux materials—particularly B_2O_3—was critical in lowering the overall melting point of the mixture and facilitating the formation of a chemically stable solid matrix. These findings demonstrate that sintering-based solidification can yield high-melting-point metal oxides with adequate chemical durability even with low glass additive contents (10–20 %), especially when using B_2O_3-rich additives. These insights offer practical guidance for formulating solidification systems that satisfy the leaching performance criteria outlined in regulatory standards. However, the present study is limited by its reliance on simulated, non-radioactive surrogates rather than actual radioactive sludge, as well as by the inherent scale constraints of laboratory testing. Additional validation under repository-relevant conditions and long-term performance assessments will be necessary to confirm the suitability of the optimized formulations for real-world application.

CRediT authorship contribution statement

Ki Joon Kang: Writing – review & editing, Writing – original draft, Visualization, Methodology, Investigation, Conceptualization. **Sia Hwang:** Writing – review & editing, Visualization, Methodology, Investigation. **Hee Reyoung Kim:** Writing – review & editing, Supervision, Project administration.

Declaration of competing interest

The authors declare that they have no known competing financial interests or personal relationships that could have appeared to influence the work reported in this paper.

Acknowledgments

This research was supported by the Korea Institute of Energy Technology Evaluation and Planning (KETEP) and the Ministry of Trade, Industry & Energy (MOTIE) of the Republic of Korea (grant no. 20214000000410), as well as by the National Research Foundation of Korea (NRF) grant funded by the Korean government (MEST) (grant no. RS-2024-00431789). The ICP-MS data were acquired using equipment provided by the UNIST Central Research Facilities (UCRF).

References

[1] Y. Cui, S. Liu, K. Smith, K. Yu, H. Hu, W. Jiang, Y. Li, Characterization of corrosion scale formed on stainless steel delivery pipe for reclaimed water treatment, Water Res. 88 (2016) 816–825, https://doi.org/10.1016/j.watres.2015.11.021.

[2] H. Provens, Primary circuit contamination in nuclear power plants: contribution to occupational exposure, in: European IRPA Congress 2002, 2002. Florence, Italy, May 8–11.

[3] J. Zhao, J.J. Zheng, G.F. Peng, K. van Breugel, Prediction of thermal decomposition of hardened cement paste, J. Mater. Civ. Eng. 24 (2011) 592–598, https://doi.org/10.1061/(ASCE)MT.1943-5533.0000423.

[4] K. Raj, K.K. Prasad, N.K. Bansal, Radioactive waste management practices in India, Nucl. Eng. Des. 236 (2006) 914–930, https://doi.org/10.1016/j.nucengdes.2005.09.036.

[5] J.F. Su, E. Schlangen, J. Qiu, Design and construction of microcapsules containing rejuvenator for asphalt, Powder Technol. 235 (2013) 563–571, https://doi.org/10.1016/j.powtec.2012.11.013.

[6] Y. Zhao, Q. Zhang, J. Chen, Y. Yi, M. Zhou, J. Cui, Effects of B_2O_3 content on crystallization behavior and properties of low temperature co-fired CaO–B_2O_3–SiO_2 glass-ceramics, J. Mater. Sci. Mater. Electron. 35 (2024) 225, https://doi.org/10.1007/s10854-024-11978-x.

[7] P. Kaushik, Indian program for vitrification of high level radioactive liquid waste, Procedia Matedr. Sci. 7 (2014) 16–22, https://doi.org/10.1016/j.mspro.2014.10.004.

[8] J.C. Marra, D.S. Kim, Towards increased waste loading in high level waste glasses: developing a better understanding of crystallization behavior, Procedia Mater. Sci. 7 (2014) 87–92, https://doi.org/10.1016/j.mspro.2014.10.012.

[9] J.M. Juoi, M.I. Ojovan, W.E. Lee, Microstructure and leaching durability of glass composite wasteforms for spent clinoptilolite immobilisation, J. Nucl. Mater. 372 (2008) 358–366, https://doi.org/10.1016/j.jnucmat.2007.04.047.

[10] K.J. Kang, S. Hwang, H.R. Kim, Reinforcement of cobalt leaching resistance of solidified sludge for disposal of radioactive sludge waste by hot isostatic pressing, J. Radioanal. Nucl. Chem. 333 (2024) 53–70, https://doi.org/10.1007/s10967-023-09247-y.

[11] P. Gibot, Templated synthesis of Cr_2O_3 material for energetic composites with high performance, Solid State Sci. 94 (2019) 162–167.

[12] National Center for Biotechnology Information, PubChem Compound Summary for CID 14805, Nickel oxide. https://pubchem.ncbi.nlm.nih.gov/compound/Nickel-oxide.

[13] M.S. Shakeri, O. Polit, B. Grabowska-Polanowska, A. Pyatenko, K. Suchanek, M. Dulski, J. Gurgul, Z. Swiatkowska-Warkocka, Solvent-particles interactions during composite particles formation by pulsed laser melting of α-Fe_2O_3, Sci. Rep. 12 (2022) 11950, https://doi.org/10.1038/s41598-022-15729-y.

[14] Z. Duan, F. Arjmand, L. Zhang, H. Abe, Investigation of the corrosion behavior of 304L and 316L stainless steels at high-temperature borated and lithiated water, J. Nucl. Sci. Technol. 53 (2015) 1435–1446, https://doi.org/10.1080/00223131.2015.1125311.

[15] A. Fomin, M. Fomina, V. Koshuro, I. Rodionov, Composite metal oxide coatings on chromium-nickel stainless steel produced by induction heat treatment, Compos. Struct. 229 (2019) 111451, https://doi.org/10.1016/j.compstruct.2019.111451.

[16] S. Kumar, P.K. Singh, D. Patel, S.B. Prasad, Optimization of TIG welding process parameters using Taguchi's analysis and response surface methodology, Int. J. Mech. Eng. Technol. 8 (2017) 932–941. https://iaeme.com/Home/issue/IJMET?Volume=8&Issue=11.

[17] H. Wang, T. Zhang, H. Zhu, G. Li, Y. Yan, J. Wang, Effect of B_2O_3 on melting temperature, viscosity and desulfurization capacity of CaO-based refining flux, ISIJ Int. 51 (2011) 702–706, https://doi.org/10.2355/isijinternational.51.702.

[18] Y.T. Fei, S.J. Fan, R.Y. Sun, J.Y. Xu, M. Ishii, Crystallizing behavior of Bi_2O_3–SiO_2 system, J. Mater. Sci. Lett. 19 (2000) 893–895, https://doi.org/10.1023/A:1006701901976.

[19] American Nuclear Society, ANSI/ANS-16.1-2019, Measurement of the Leachability of Solidified Low-Level Radioactive Wastes by a Short-Term Test Procedure, American Nuclear Society, La Grange Park, IL, 2019.

[20] B.C. Bunker, G.W. Arnold, D.E. Day, P.J. Bray, The effect of molecular structure on borosilicate glass leaching, J. Non-Cryst. Solids 87 (1986) 226–253, https://doi.org/10.1016/S0022-3093(86)80080-1.

[21] N.A. Mayer, D.M. Cupid, R. Adam, A. Reif, D. Rafaja, H.J. Seifert, Standard enthalpy of reaction for the reduction of Co_3O_4 to CoO, Thermochim. Acta 652 (2017) 109–118, https://doi.org/10.1016/j.tca.2017.03.011.

[22] J. Liu, J. Baeyens, Y. Deng, X. Wang, H. Zhang, High temperature Mn_2O_3/Mn_3O_4 and Co_3O_4/CoO systems for thermo-chemical energy storage, J. Environ. Manag. 267 (2020) 110582, https://doi.org/10.1016/j.jenvman.2020.110582.